Cancer Research

Darwinian Dynamics of Intratumoral Heterogeneity: Not Solely Random Mutations but Also Variable Environmental Selection Forces

Mark C. Lloyd[1,2], Jessica J. Cunningham[3], Marilyn M. Bui[3,4], Robert J. Gillies[3], Joel S. Brown[2], and Robert A. Gatenby[5,6]

Abstract

Spatial heterogeneity in tumors is generally thought to result from branching clonal evolution driven by random mutations that accumulate during tumor development. However, this concept rests on the implicit assumption that cancer cells never evolve to a fitness maximum because they can always acquire mutations that increase proliferative capacity. In this study, we investigated the validity of this assumption. Using evolutionary game theory, we demonstrate that local cancer cell populations will rapidly converge to the fittest phenotype given a stable environment. In such settings, cellular spatial heterogeneity in a tumor will be largely governed by regional variations in environmental conditions, for example, alterations in blood flow. Model simulations specifically predict a common spatial pattern in which cancer cells at the tumor–host interface exhibit invasion-promoting, rapidly proliferating phenotypic properties, whereas cells in the tumor core maximize their population density by promoting supportive tissue infrastructures, for example, to promote angiogenesis. We tested model predictions through detailed quantitative image analysis of phenotypic spatial distribution in histologic sections of 10 patients with stage 2 invasive breast cancers. CAIX, GLUT1, and Ki67 were upregulated in the tumor edge, consistent with an acid-producing invasive, proliferative phenotype. Cells in the tumor core were 20% denser than the edge, exhibiting upregulation of CAXII, HIF-1Î±, and cleaved caspase-3, consistent with a more static and less proliferative phenotype. Similarly, vascularity was consistently lower in the tumor center compared with the tumor edges. Lymphocytic immune responses to tumor antigens also trended to higher level in the tumor edge, although this effect did not reach statistical significance. Like invasive species in nature, cancer cells at the leading edge of the tumor possess a different phenotype from cells in the tumor core. Our results suggest that at least some of the molecular heterogeneity in cancer cells in tumors is governed by predictable regional variations in environmental selection forces, arguing against the assumption that cancer cells can evolve toward a local fitness maximum by random accumulation of mutations. *Cancer Res; 76(11); 3136–44. ©2016 AACR.*

Major Findings

Like invasive species in nature, cancer cells at the leading edge of the tumor possess a different phenotype from cells in the tumor core. We conclude that at least some intratumoral heterogeneity in the molecular properties of cancer cells is governed by predictable regional variations in environmental selection forces.

[1]Inspirata Inc. One North Dale Mabry, Tampa, Florida. [2]Department of Biological Sciences, University of Illinois, Illinois, Chicago. [3]Department of Cancer Imaging and Metabolism, H Lee Moffitt Cancer Center and Research Institute, Tampa, Florida. [4]Department of Pathology, H Lee Moffitt Cancer Center and Research Institute, Tampa, Florida. [5]Department of Integrated Mathematical Oncology, H Lee Moffitt Cancer Center and Research Institute, Tampa, Florida. [6]Department of Radiology, H Lee Moffitt Cancer Center and Research Institute, Tampa, Florida.

Note: Supplementary data for this article are available at Cancer Research Online (http://cancerres.aacrjournals.org/).

M.C. Lloyd and J.J. Cunningham contributed equally to this article.

Corresponding Author: Robert A. Gatenby, H. Lee Moffitt Cancer Center and Research Institute, 12902 Magnolia Drive, SRB 24000E, Tampa, FL 33612. Phone: 813-745-2843; Fax: 813-745-6070; E-mail: robert.gatenby@moffitt.org

doi: 10.1158/0008-5472.CAN-15-2962

Introduction

Although patient-specific, precision therapy remains an important goal in oncology, treatment strategies based on static and non-spatial data can be limited as somatic evolution continuously alters the tumor environments and cell populations over space and time (1). For example, recent studies demonstrate significant intratumoral spatial heterogeneity in the molecular properties of cancer cells in several tumor types (2–4). These regional variations are widely recognized as evidence of intratumoral evolution, but the proposed dynamics typically focus on random acquisition of mutations that confer a fitness advantage resulting in a "selective sweep" (5, 6) by the new population. An important clinical implication of this conventional "clonal branching" model is that intratumoral molecular heterogeneity, because it is dependent on stochastic accumulation of mutations, must be fundamentally unpredictable.

An implicit assumption of conventional models of intratumoral evolution is that cancer cells do not achieve a fitness maximum so that cancer cells can always undergo mutations that increase their fitness allowing a new population to emerge even within a static environment. In contrast, we note that very different dynamics will results if tumor cells, like most species in nature, rapidly evolve to local fitness maximum (7) so that no heritable change can further increase its fitness. In fact, under such conditions, the population will tend converge to a single dominant

Quick Guide to Equations and Assumptions

Darwinian dynamics of intratumoral heterogeneity

The fitness generating function is given by

$$G(u,\ u,\ x_A,\ x_B)\ =\ pF_A + (1-p)F_B.$$

The fitness of a focal individual in a habitat $i = A\ or\ B$ of species j is a function of its strategy u and the current density of individuals within that habitat x_i given by

$$F_i(u,\ u,\ x_i)\ =\ r_i(u)\left(\frac{K_i(u) - \sum_j x_{ij}}{K_i(u)}\right) - d_i.$$

The individuals' strategy u within a habitat affects both the logistic growth rate and carrying capacity given by

$$r_i(u)\ =\ r_{i0}\exp\left(-\frac{(u-1)^2}{\sigma_K^2}\right)\ \text{and}\ K_i(u)\ =\ k_{i0}\ \exp\left(-\frac{u^2}{\sigma_K^2}\right).$$

A strategy u will converge on a distribution of individuals among habitats such that the strategy has the same per capita growth rate in each habitat. Equilibrating $\frac{\partial x_{ij}}{\partial t}$ and substituting $q = x_A/x_B$ results in

$$q\ =\ \frac{(F_A -\ F_B + m_B - m_A) + \sqrt{(F_B - F_B + m_A - m_B)^2 + 4m_A m_B}}{2m_A}.$$

Therefore, the frequency with which a strategy u will eventually experience habitat A for any fixed biotic environment is given by

$$p(u,\ u,\ x_A,\ x_B)\ =\ \frac{q}{(q+1)}.$$

The population dynamics of the size of a species within a habitat is given by

$$\frac{\partial x_{ij}}{\partial t}\ =\ x_{ij}\ \times\ [F_i(u_j,\ u,\ x_i) - m_i x_{ij} + m_l x_{lj}],\ l \neq i.$$

The strategy dynamics is given by

$$\frac{\partial u}{\partial t}\ =\ C\ \times\ \frac{\partial G}{\partial u}.$$

Together, the population dynamics and the strategy dynamics represent the complete Darwinian dynamics of the system. The ecologic and evolutionary dynamics generally converge on an "evolutionary stable strategy" (ESS). At an ESS the system becomes both ecologically $[\partial x/\partial t = 0]$ and evolutionarily stable $[\partial G/\partial v = 0]$.

Parameters

- c is a constant that scales the speed of evolutionary change;
- d_i is an extrinsic mortality term not built into the logistic growth due to ecologic properties of the habitat;
- r_{i0} is the maximum growth rate of each habitat $i = A\ or\ B$;
- k_{i0} is the maximum carrying capacity of each habitat $i = A\ or\ B$;
- σ_K^2 is a constant characterizing the Gaussian penalty due to strategy to $r_i(u)$ and $K_i(u)$;
- m_i is the per capita migration rate of individuals from habitat i to the alternate habitat l for $l \neq i$;

Major Assumptions

1 Species are identical in all ways except for the values of their strategies.
2 The strategy u represents investment along a continuum of all CAIX ($u = 0$) and all CAXII ($u = 1$).
3 A tradeoff exists between fitness in the two habitats, where $\partial F_A/\partial u > 0$ and $\partial F_B/\partial u < 0$.
4 There are diminishing returns in fitness in habitat A from increasing u and to fitness in B from decreasing u, where $\partial^2 F_A/\partial u^2 < 0$ and $\partial^2 F_B/\partial u^2 < 0$.
5 Individuals compete with each other for limiting resources within each habitat, so fitness within a habitat declines with an increase of individuals within that habitat, where $\partial F_A/\partial x_A < 0$ and $\partial F_B/\partial x_B < 0$.
6 Migration rates m_A and m_B are passive in that we assume that m_A and m_B are independent of strategies, u, and species population sizes, x_A and x_B.

phenotype, resulting in decreasing heterogeneity. Thus, in this alternative model of cancer evolution, spatial variation of phenotypes must result from local variations in environmental factors that select for different phenotypic properties. For example, regions of low blood flow, a common observation in tumor imaging, will select for tumors that are optimally adapted to environmental conditions that include reduced availability of substrate and blood-derived growth factors. Importantly, in contrast with the conventional model, this approach requires molecular characteristics of cancer cells to be non-random. That is, the local phenotypic properties of cancer cells should be generally predictable with sufficient understanding of local environmental properties and Darwinian dynamics (8).

Here, we frame this hypothesis using mathematical models from evolutionary game theory (9, 10). The quantitative methods extend prior work that applied classic evolutionary trade-offs between fecundity and survivorship. That is, we propose cancer cells, like all evolving organisms, can invest resources to maximize fecundity or survivorship but not both (11). This Darwinian trade-off manifests in cancer cells as two tumor cell types roughly correspond to what is known as *r* and *K* selection (12) where "*r*" refers to a species with maximal growth rate (capacity to grow at low population densities) as opposed to "*K*" referring to a species that maximizes its carrying capacity (capacity to maintain growth at high population densities).

Although based on simple evolutionary first principles, the model leads to complex and variable spatial and temporal population. However, we find that the model does consistently predict one property of the tumor ecology—that the cancer cells at the tumor–host interface will demonstrate phenotypic properties that are consistent between tumors, but very different from the properties of cells deeper within the same tumor. We then examine model predictions through detailed, quantitative analysis of spatial distribution of phenotypic properties in histologic sections taken from 10 patients with stage 2 invasive breast cancers.

Materials and Methods

All clinical components of the study were completed with the approval of the University of South Florida Institutional Review Board. Participant's written consent was not obtained because all personal health information was de-identified and analyzed anonymously. The Moffitt Scientific Review Committee and University of South Florida IRB committee both approved this protocol (MCC 16511).

Mathematical model

We investigate a mathematical model from evolutionary game theory of habitat heterogeneity (12), in which we envision two habitats, the core of the tumor versus the tumor edge. We assume that cancer cells can evolve whereas normal cells do not. However, normal mesenchymal cells retain phenotypic plasticity and may be influenced and/or co-opted by the tumor cells to generate a tissue infrastructure that favors cancer growth. Within a habitat, we assume that the cancer cells compete for limiting resources but do not interact directly with cells in the other habitat. Indirectly, however, their habitats do interact via migration where a fraction of the population form each habitat actively moves into the adjacent habitat or find themselves in that habitat as the edge of the tumor either recedes, expands or shifts location.

We imagine an evolutionary strategy that represents a trade-off between capacities to produce carbonic anhydrase (CA), CAXII versus CAIX. CAIX and XII are extracellular enzymes that catalyze the reversible hydration of CO_2 to bicarbonate and a proton:

$$CO_2 + H_2O \leftrightarrow HCO_3^- + H^+$$

CAIX is a transmembrane glycoprotein whose catalytic domain faces the extracellular milieu (13). CAXII has a similar overall secondary structure and orientation to CAIX, although missing the PG-like domain. CAIX sets the extracellular pH at 6.8 whereas CAXII sets the extracellular pH at 7.4. We use this difference in extracellular pH set point as markers for phenotypic strategy. It is also reported that CAIX is a poor prognostic indicator and CAXII is a positive prognostic indicator in breast cancer (14).

The buffering and habitat modulating properties of CAXII promotes or are associated with higher carrying capacity (K) and lower maximum proliferation rates (r)—such a species emphasizing CAXII is "*K*-selected." The acid-tolerating properties of CAIX promotes or are associated with resistance to the immune system, degradation of normal cells, and higher proliferation rates—such a species is "*r*-selected." We scale the heritable strategy, u, to range from $u = 0$ (maximum carrying capacity K and minimum growth rate r) to $u = 1$ (minimum K and maximal r).

Via competition within habitats and migration between habitats, the tumor cells engage in an evolutionary game in which an individual's fitness, $G(u,\ u,\ x_A,\ x_B)$, depends upon its strategy, u, the strategies of the other tumor cells, u, and population sizes of tumor cells in the interior (A) and edge (B) of the tumor, x_A and x_B, respectively. The evolutionary dynamics of the cancer cell strategies can be visualized on an adaptive landscape. This landscape plots G versus the strategy of the focal individual, u. The adaptive landscape is fixed for a given tumor population with its associated strategies and population sizes. But, as the populations' strategies evolve (evolutionary dynamics) and their associated population sizes change (ecological dynamics) the landscape also changes. Hence, the landscape itself is dynamic in response to the Darwinian dynamics of strategies and population sizes (15). At any time and point along this landscape the population will evolve "uphill" until it reaches a convergent stable point—at this point, the slope of the landscape is zero ($\partial G/\partial v = 0$), and the population sizes equilibrate so that fitness is 0 ($G = 0$). This convergent stable point can either be at a maximum or minimum of the adaptive landscape (16). If at a maximum, then the cancer has evolved to its evolutionarily stable strategies (ESS) and such a state will be both ecologically and evolutionarily persistent. If at a minimum, then the cancer cell population is under strong disruptive selection and it should "speciate" into two distinct clades that diverge and evolve to occupy distinct niches seen as distinct peaks of the adaptive landscape (17).

Further methods, details, and theories of the game theory model and image analysis strategies may be found in Supplementary Material.

Case selection

Following approval by the Institutional Review Board, 10 patients with formalin-fixed and paraffin-embedded (FFPE) blocks of diagnosed invasive ductal breast carcinoma were retrospectively examined. Cases were selected by a practicing pathologist (M.M. Bui) to include five each of the three Nottingham score grades.

Histology

Sectioning. The Tissue Core at Moffitt located each FFPE block and 4-μm serial slides from each patient were sectioned using standard histotechnique.

Immunohistochemical staining

Slides were stained using a Ventana Discovery XT automated system (Ventana Medical Systems) as per the manufacturer's protocol with proprietary reagents. Slides were deparaffinized on the automated system with EZ Prep solution (Ventana).

For the CD34 staining, the mouse monoclonal antibody CMA334 (Cell Marque) was used at a prediluted concentration and incubated for 16 minutes. The Ventana OmniMap anti-mouse secondary antibody was incubated for 12 minutes. Ventana ChromoMap was used for detection.

For the KI67 staining, the rabbit primary antibody #790-4286 (Ventana) was applied and incubated for 16 minutes. The Ventana anti-rabbit secondary was incubated for 16 minutes. The detection system was OmniMap.

To stain for CAIX, the rabbit primary antibody #ab15086 (Abcam) was used at a 1:500 concentration in Dako antibody diluent and incubated for 32 minutes. The OmniMap anti-rabbit secondary was used for 20 minutes. ChromoMap was used for detection.

For CAXII, the rabbit primary antibody #HPA008773 (Sigma) was used at a 1:75 concentration in Dako antibody diluent and incubated for 32 minutes. The OmniMap anti-rabbit secondary was used for 20 minutes. The detection system was ChromoMap.

Each set was counter stained with hematoxylin then dehydrated and coverslipped per standard histologic protocol.

Imaging and analysis

Image acquisition. Stained slides were digitally scanned using the Aperio (Vista) ScanScope XT high-throughput slide scanning instrument (200×/0.75NA objective with a rate of 2–3 minutes per slide via Basler tri-linear array).

Segmentation. Histology pattern recognition technology used included both Aperio's GENIE software and Definiens (Munich, Germany) TissueStudio v3.0 to identify tumor regions of interest (26, 27). Regions of the tumor edge were defined as areas within 1 mm of the tumor–host interface and tumor center regions were defined as any area deeper than 1 mm of the tumor–host interface. For each measurement a 500 × 500 μm subregion was randomly selected using a custom Matlab (R2014b) script. Three subregions were used for each analysis of the center or edge regions for each patient sample. Furthermore, single cells were identified as tumor and mesenchymal regions, respectively, by identifying the nuclei and growing cell simulations 5 μm. The classified nuclear and cytoplasmic subcellular compartments were evaluated independently for biomarkers that localize to a specific cellular region. Intensity thresholds from each biomarker were determined by the study pathologist (M.M. Bui) and retained consistently for each patient set.

Results

Cancer adaptive landscapes and intratumoral evolution

Although tumors likely possess a large number of ecologic niches, our model simulations focused on just two: (i) the tumor–host interface in which tumor cells compete primarily interact with elements of normal tissue, including the predatory effects of the immune response and normal tissue infrastructure such as intact blood vessels and (ii) the interior in which tumor cells compete with each other and must actively promote formation of the mesenchymal infrastructure required to support the population.

If the population of tumor cells is well-mixed between edge and interior of the tumor (high migration rate, m), then evolution promotes an ESS that is a single clone (Fig. 1). This clone possesses a generalist strategy balancing the need for a higher r when facing the edge habitat and a higher K when facing the interior. No matter the starting strategy of the population, it will evolve toward the same peak of the adaptive landscape. We expect this outcome when either the spatial heterogeneity of habitat types is very fine grained, or the cells for some reason are highly motile and frequently move from one habitat to the next, which itself could be a response to environmental selective pressures (18). For larger more advanced tumors, we would expect edge and interior habitats to be more coarse grained, and the likelihood of a given tumor cell moving from one to the other to be relatively small on a per 8 to 24 hours basis (the likely unit of time in our model).

If the migration rate is small, an axis of heterogeneity describing the edge to interior of the tumor can result in the speciation of a single clonal cancer lineage into two distinct phenotypes specialized to exploit different regions of tumor heterogeneity (Fig. 2). If the tumor starts with a single evolving population of cancer cells, then these cells evolve up the slope of the adaptive landscape. But instead of achieving a peak, they actually evolve to an evolutionarily stable minimum on the landscape. At this point, disruptive selection should promote speciation and the divergence of

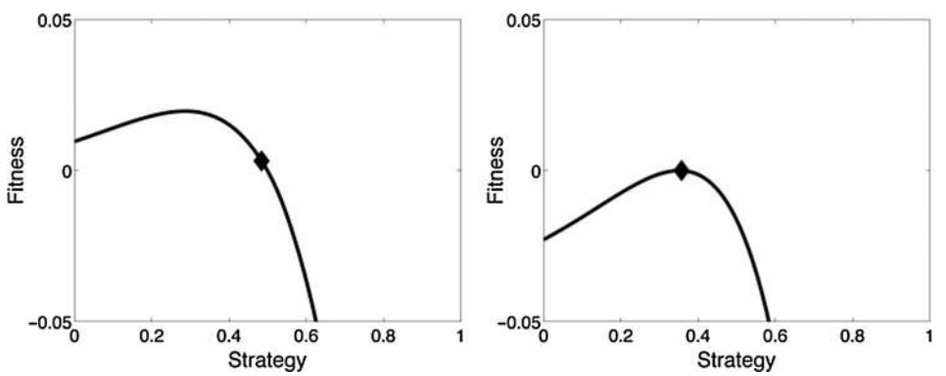

Figure 1.
Evolution of a population of cells in an environment where the migration rate is high ($m = 0.1$). The initial population begins with a strategy $u = 0.5$ (left). Evolutionary dynamics will cause this population's strategy to climb the adaptive landscape. Through both the ecological and evolutionary dynamics, an ESS is achieved at a strategy of $u = 0.3564$ (right).

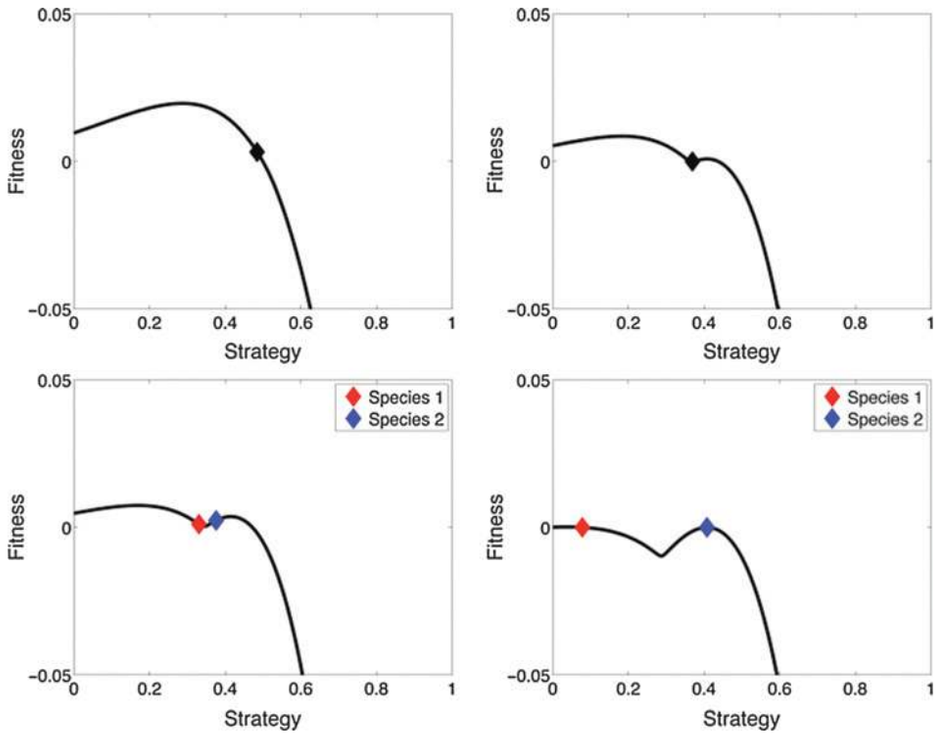

Figure 2.
Evolution of a population of cells in an environment where the migration rate is low ($m = 0.001$). Again, the initial population begins with a strategy of $u = 0.5$ and begins to climb the adaptive landscape (top left). Instead of achieving a peak, the population actually evolves to an evolutionarily stable minima of the landscape at $u = 0.3677$ (top right). Disruptive selection causes the single population to diverge into two separate species. The one being K-selected is shown as species 1 in red and evolves to an ESS of $u = 0.0774$. The other being r-selected is shown as species 2 in blue and evolved to an ESS of $u = 0.4074$ (bottom).

separate tumor cell types. The one being *K*-selected (CAXII) and the other *r*-selected (CAIX). Although some spatial overlap will occur between the two types, the former will predominate in the interior of the tumor and the latter at the tumor's edge.

More generally the model shows how the grain-size of habitat heterogeneity and the motility of tumor cells will determine whether tumor heterogeneity promotes generalist versus more specialist tumor "species." Figure 3 shows how low migration rates promote speciation and divergent strategies among the tumor cells. As the migration rate increases, the values of the two strategies comprising the ESS begin to converge and do so at a critical threshold value of migration. At higher rates of migration above this threshold, the ESS is a single species with a generalist strategy (Fig. 3).

In summary, the model simulations demonstrate that selection forces in the tumor core favor tumor cells with "engineering" phenotypes that maximize carrying capacity by promoting angiogenesis and aggressively competing for limited resources. Conversely, the tumor cells at the leading edge (i.e., the tumor-host interface) possess "pioneering" phenotypes that maximize their invest resources in invasive strategies that permit them to acquire resources through co-opting normal vessels and other host mesenchyma even at the expense of a potentially higher death rate due to host response. Thus, in general our models predict "engineering" phenotypes will dominate the tumor core whereas cells at the leading edge of tumor will exhibit phenotypes that can pioneer in a novel, and sometimes hostile environment. Interestingly, this prediction is consistent with observations in nature that "weedy" phenotypes (i.e., higher maximum proliferation rates at the expense of lower carrying capacities) predominate at the leading edge of a population invasion when compared with individuals in regions far from the propagating border (19).

Clinical analysis

As described above, the evolutionary models predict observable changes in the neoplastic cells and the environment in both the center and edge regions of a tumor. We tested these model predictions with clinical analysis of histologic sections evaluated by quantitative image analysis. Our clinical results indicate a number of consistently observed and quantified changes in cell

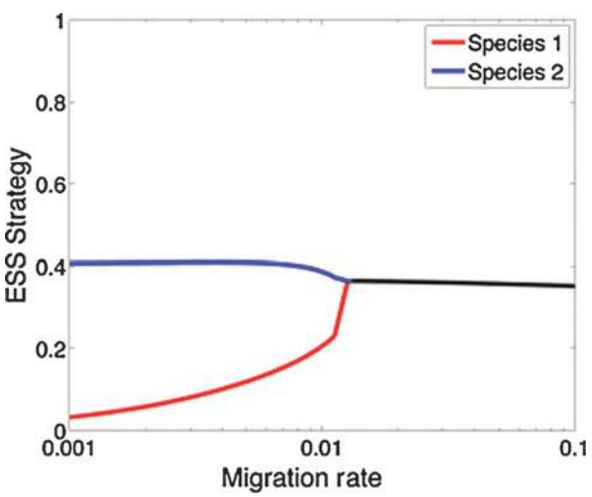

Figure 3.
Evolutionary stable strategies versus the migration rate *m*. Speciation into two distinct strategies occurs at low migration rates ($m < 0.012$). At high migration rates ($m > 0.012$), the values of the two strategies converge to a single species with a generalist strategy. The dynamics of $m = 0.1$ are shown in Fig. 1 and the dynamics of $m = 0.001$ are shown in Fig. 2.

Table 1. Statistical summary for each biomarker by region interaction

	Multiple r^2	F-ratio (habitats)	F-ratio (patients)	F-ratio (habitats*patients)	*P* (habitats)	*P* (patients)	*P* (habitats*patients)
Cell density	0.072	15.387	9.297	0.495	<0.0001	<0.0001	n.s.
CAIX	0.908	255.766	7.881	4.513	<0.0001	<0.0001	0.001
CAXII	0.927	329.297	12.495	3.318	<0.0001	<0.0001	0.006
KI67	0.88	73.58	21.559	1.516	<0.0001	<0.0001	n.s.
CC3	0.838	45.231	12.036	5.993	<0.0001	<0.0001	<0.0001
Glut1	0.933	148.704	22.081	1.692	<0.0001	<0.0001	n.s.
HIF-1α	0.861	13.4	24.44	1.516	0.001	0.001	n.s.
CD34 (#)	0.797	22.482	12.661	2.261	<0.0001	<0.0001	n.s.
CD34 (#)	0.64	27.25	2.886	1.692	<0.0001	0.014	n.s.
Lymphocytes	0.793	0.057	14.708	2.744	0.812	<0.0001	n.s.

Abbreviation: n.s., nonsignificant.

density, cell proliferation, cell death, cell aggression, acidosis, and hypoxia in both locations (each measured in triplicate) of histologic samples of 10 invasive breast cancer patients. Furthermore, the presence of lymphocytes and vascular resources in the microenvironment were measured in triplicate in both locations of the same tumors (See Table 1 and Fig. 4).

First, the tumor cell density was evaluated. We used a partially hierarchical ANOVA (SYSTAT version 13) to test for the effects of tumor cell density (number of tumor cells per area) and habitat (tumor center vs. tumor edge; each with triplicate sampling) for each of 10 patients. These analyses were calculated by quantifying the number events (as indicated as the number of tumor cells or, for each biomarker, strongly expressing tumor cells) within a 500 by 500 μm subregion. Each subregion was extracted randomly, in triplicate, from within 1 mm of the mesenchymal interface for edge samples and beyond 1 mm from the mesenchymal interface for center regions. The cell density model provided a good fit to the data (multiple $r^2 = 0.72$). The patient [F-Ratio = 0.49, not significant (n.s.)] was not found to influence the ratio of cell counts per region so that the tissue slices provided roughly the same ratio of cancer cells regardless of patient. Cancer cell abundances varied significantly by center and edge region (F-Ratio = 15.39, $P < 0.001$) for all patients (F-Ratio = 9.20, $P < 0.001$). This indicates that cells in the tumor center out-numbered cells at the tumor edge consistently across all patients with statistical significance.

Second, the tumor cell proliferation was evaluated by evidence of Ki-67 expression across tumor cells in triplicate for both regions for the same 10 patients. The model also provided a good fit to the data (multiple $r^2 = 0.88$). Again the patient (F-Ratio = 2.74, n.s.) was not found to influence the ratio of Ki67-positive cells per region so that the tissue slices provided roughly the same ratio of Ki67 positivity regardless of patient. Proliferation varied very significantly by center and edge region (F-Ratio = 73.58, $P < 0.001$) for all patients (F-Ratio = 21.56, $P < 0.001$). This indicates that proliferative cells in the tumor edge consistently out-numbered cells in the tumor center across all patients with statistical significance.

Next, the tumor cell death by apoptosis was evaluated by evidence of cleaved caspase-3 (CC3) expression across tumor

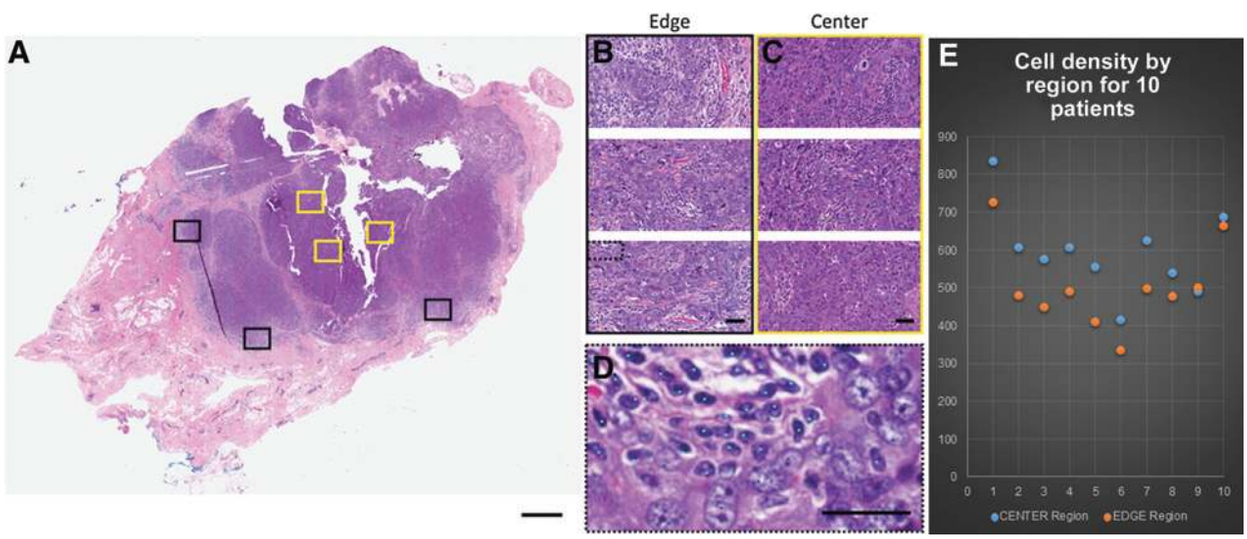

Figure 4.
H&E images of a grade 3 invasive breast cancer. A, regions were randomly selected from the whole slide image, such that three regions were within 1 mm of the edge of the tumor border (black boxes) and three regions were located near the center of the tumor region (yellow boxes). Scale bar, 2 mm. B and C, Each edge region (B) and each center region (C) are shown at ×200 magnification; scale bar, 100 μm. D, digitally zoomed to ×1,000 from the dotted black box and demonstrates the tumor cell identification (blue points) and lymphocyte identification (teal points) used to calculate both the tumor cell density and lymphocyte numbers in each of the 60 H&E and 600 total images evaluated; scale bar, 100 μm. E, scatter plot of the 10 patient's (*x*-axis) cell density (*y*-axis) for the center (blue) and edge (orange) regions.

cells in triplicate for both regions for the same 10 patients. The model also provided a good fit to the data (multiple $r^2 = 0.84$). Here, CC3 expression varied very significantly by center and edge region (F-Ratio = 45.23, $P < 0.001$) for all patients (F-Ratio=12.04, $P < 0.001$). This indicates that apoptosis in the tumor center consistently out-numbered cells in the tumor edge across all patients with statistical significance.

Then, a number of additional metabolomic biomarkers that indicate tumor cell aggression, acidosis, glycolysis, and hypoxia were tested. Aggressive, acid producing cells should be consistently observed in the tumor edge whereas cells in vascularized regions of the remainder of the tumor should be functioning in normal pHe. To test model predictions, we examined the spatial distribution of CAIX and XII as biomarkers for regional high and low acidity, respectively.

The model provided a good fit to the CAIX data (multiple $r^2 = 0.91$) and the CAXII data (multiple $r^2 = 0.93$). CAIX expression varied very significantly by center and edge region (F-Ratio = 255.77, $P < 0.001$) for all patients (F-Ratio = 7.88, $P < 0.001$) whereas CAXII expression varied very significantly by center and edge region (F-Ratio = 329.27, $P < 0.001$) for all patients (F-Ratio = 12.50, $P < 0.001$). This indicates that CAIX-expressing cells in the tumor edge consistently out-numbered cells in the tumor center across all patients with statistical significance when the converse is true of CAXII, which consistently has higher expression in the tumor center across all patients with statistical significance. This matched with the predictions of the evolutionary mathematical models (Fig. 5).

Glycose transporter 1 (GLUT1), also known as solute carrier family 2 facilitated glucose transporter member 1 (SLC2A1; multiple $r^2 = 0.93$) and hypoxia-inducible factor 1-alpha (HIF1α; multiple $r^2 = 0.86$) measurements were similarly modeled. GLUT1 expression varied very significantly by center and edge region (F-Ratio = 148.70, $P < 0.001$) for all patients (F-Ratio = 22.08, $P < 0.001$) whereas HIF1α expression varied very significantly by center and edge region (F-Ratio = 13.40, $P = 0.001$) for all patients (F-Ratio = 24.44, $P < 0.001$). This indicates that GLUT1-expressing cells in the tumor edge consistently out-numbered cells in the tumor center across all patients with statistical significance when the converse is true of HIF1α, which consistently has higher expression in the tumor center across all patients with statistical significance.

Finally, two aspects of the environment were quantified: The vascular density (number and area of vasculature) and the density of lymphocytes per region area. The number of blood vessels per area (multiple $r^2 = 0.80$), the area of vascular involvement (multiple $r^2 = 0.77$) and the density of lymphocytes (multiple $r^2 = 0.79$) were modeled. The number of blood vessel per area varied significantly by center and edge region (F-Ratio = 22.48, $P < 0.001$) for all patients (F-Ratio = 12.66, $P < 0.001$) whereas the area of vascular involvement varied significantly by center and edge region (F-Ratio = 16.85, $P < 0.001$) for all patients (F-Ratio = 11.62, $P < 0.001$) whereas lymphocytic density did not vary significantly by center and edge region (F-Ratio = 0.057, n.s.) but was consistent for all patients (F-Ratio = 14.71, $P < 0.001$). This indicates that the number and area of vasculature was statistically greater at the tumor edge than in the tumor center across all patients; however, the lymphocytes were statistically similar in both the edge and center regions across all patients. Non-specific staining of one of the patients may have resulted in an artificially high patient interaction effect. When this patient's samples were removed the trend remained constant for the center to edge effect (F-Ratio = 27.25, $P < 0.001$) and the patient effect was reduced to (F-Ratio = 2.89, n.s.). The lymphocytic response, taken together with the tumor cell density does, however, indicate that the ratio of lymphocytes to tumor cells is consistently high at the tumor edge (where the tumor cell density is lower than the center).

Overall, the biomarker measures of tumor cells are strikingly segregated by center and edge regions. This species by habitat interaction contributes most to the explained variation within the statistical model (see Table 1 for a statistical summary for each biomarker by region interaction). See Fig. 6 for a graphical representation of each data point.

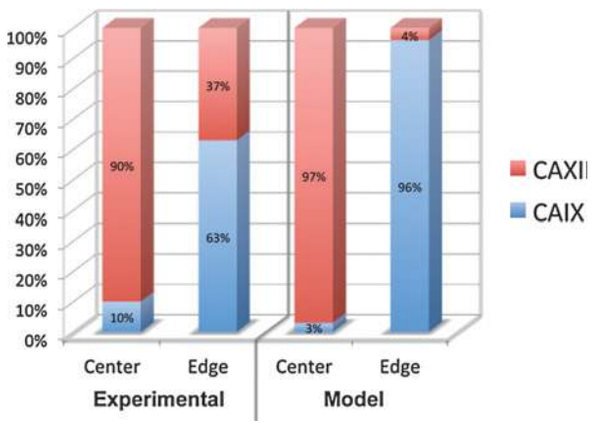

Figure 5.
Experimental and mathematical model results showing the percentage of total cells counted in the center and edge that expressed either CAIX or CAXII. Experimental results showed that 90% of the cells in the center of the tumors expressed CAXII, whereas only 10% expressed CAIX. Conversely, 63% of the cells in at the edge of the tumors expressed CAIX. The mathematical model showed that 97% of the cells in the center would express CAXII and 96% of the cells at the edge would express CAIX.

Discussion

The conventional model of intratumoral evolution allows new "driver" mutations to accumulate indefinitely, resulting in branching clonal evolution. This conceptual model implicitly assumes that tumor cells never achieve a local fitness maximum so that new mutations can always generate a novel (and fitter) genotype and phenotype. Here, we explore an alternative model in which cancer cells may evolve to an evolutionary stable state (ESS) and, thus, cannot be displaced by new strategies if the environment remains stable. This would lead to local phenotypic convergences so that regional molecular variations, rather than the result of random mutations, would represent reasonably predictable phenotypic adaptations to changes in environment conditions such as blood flow, as described in the results, and via conventional clinical imaging such as MRI. This model would be supported by identification of a simple, consistent spatial variation in tumor molecular properties that emerged directly from fundamental evolutionary dynamics.

Here, we framed this hypothesis mathematically using evolutionary game theory. Although built on a simple conceptual model, computer simulations demonstrate the ecological dynamics within cancers can be quite complex and highly variable from

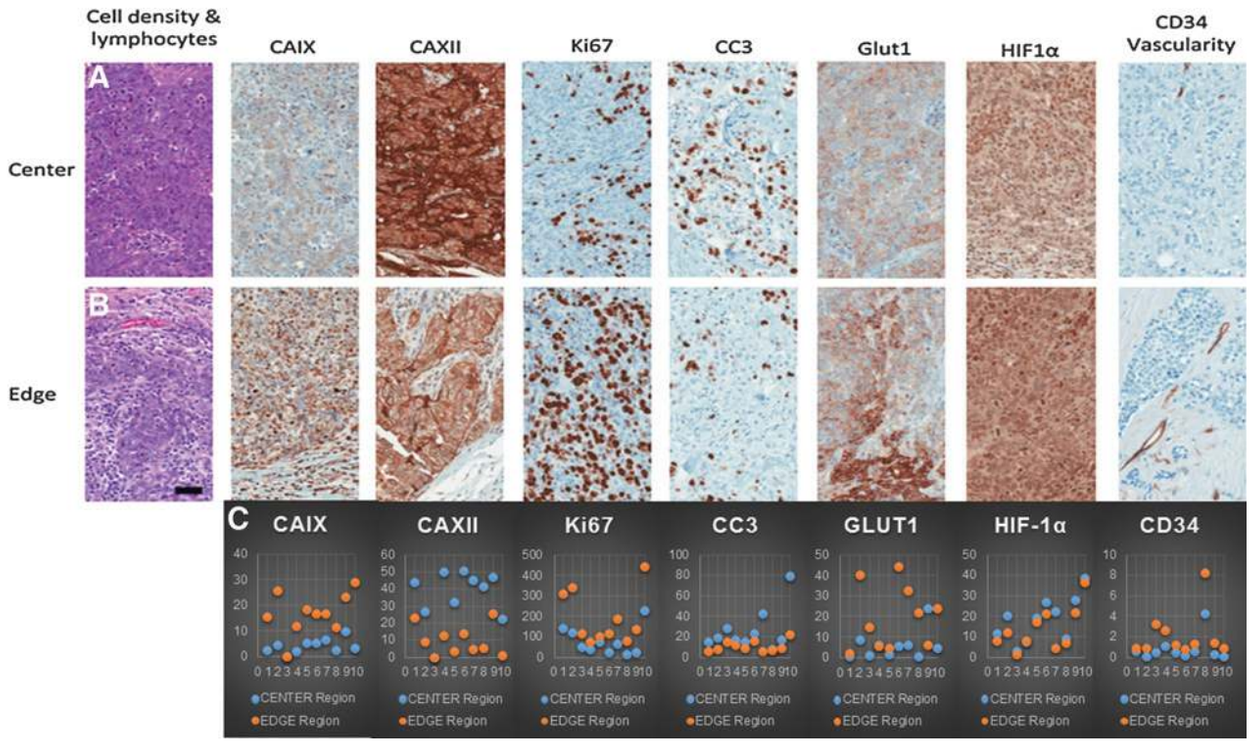

Figure 6.
Comparison of tumor cell molecular properties at the invasive edge compared with the tumor core. A and B, an image panel of center (top; A) and edge (bottom; B) regions are displayed to demonstrate examples of each biomarker staining within each area of interest; scale bar, 100 μm. C, scatter plot of the 10 patient's (*x*-axis) CAIX, CXII, Ki67, CC3, GLUT1, HIF-1α, and CD34 biomarkers for the center (blue) and edge (orange) regions.

tumor to tumor. However, a common pattern emerged as our models predicted cancer cells at the invasive front of the tumor will consistently possess distinct phenotypic properties when compared with the cells in the core. Interestingly, similar patterns of distinctive phenotypes at the leading edge have been observed in biological invasions such as the cane toad in Australia (20) and the house sparrow in Kenya (21).

Detailed analysis of spatial molecular heterogeneity in 10 clinical breast cancers demonstrates a consistent regional distribution in which proliferation, the ratio of tumor cells to lymphocytes, GLUT1 and CAIX expression were higher at the tumor edge. Conversely, tumor cell density, apoptosis, HIF1α and CAXII expression were observed to be greater in the tumor center. We also investigated the location of increased vascularity and cell death. Although the number of clinical tumors is small, we note that the results are highly statistically significant. Furthermore, other clinical studies have observed changes in gene expression in the edge of cutaneous squamous cell carcinoma (22, 23) and colon cancer (24).

Our results are similar to the variations in favorable and unfavorable gene signatures within the same tumor reported in prior studies (1, 3). For example, our results show that positive prognostic (CAXII) and negative prognostic (CAIX) biomarkers are routinely observed in the same tumor but different regions. Importantly, however, we can clearly identify the Darwinian dynamics that produced this spatial variation, and thus place this regional heterogeneity within an ecologic and evolutionary context. This may have clinical implications because it supports the hypothesis that at least some intratumoral heterogeneity in the molecular properties of cancer cells can be predicted on the basis of the local environmental selection forces, which can be defined by clinical imaging (25–27).

Our results suggest a number of important avenues for future investigation. Because clinical cancer imaging can depict spatial variations in perfusion, it should be possible to estimate some molecular variations based on imaging. In addition, it seems clear that some current prognostic and predictive molecular biomarkers that can be observed in different regions of the same tumor, such as CAIX and CAXII, can be accurately evaluated and reported only in a spatial context.

Disclosure of Potential Conflicts of Interest

R.J. Gillies has ownership interest (including patents) and is a consultant/advisory board member for Health Myne. No potential conflicts of interest were disclosed by the other authors.

Authors' Contributions

Conception and design: M.C. Lloyd, J.J. Cunningham, M.M. Bui, R.J. Gillies, J.S. Brown, R.A. Gatenby

Development of methodology: M.C. Lloyd, J.J. Cunningham, J.S. Brown, R.A. Gatenby

Acquisition of data (provided animals, acquired and managed patients, provided facilities, etc.): M.C. Lloyd, J.J. Cunningham, M.M. Bui, R.A. Gatenby

Analysis and interpretation of data (e.g., statistical analysis, biostatistics, computational analysis): M.C. Lloyd, J.J. Cunningham, M.M. Bui, R.J. Gillies, J.S. Brown, R.A. Gatenby

Writing, review, and/or revision of the manuscript: M.C. Lloyd, J.J. Cunningham, M.M. Bui, R.J. Gillies, J.S. Brown, R.A. Gatenby

Administrative, technical, or material support (i.e., reporting or organizing data, constructing databases): M.C. Lloyd
Study supervision: J.S. Brown, R.A. Gatenby

Acknowledgments

The authors would like to extend their most sincere thanks to all of those who discussed, reviewed, and provided edits for this article, especially Tamir Epstein and the Brown laboratory. The authors thank the Moffitt Tissue Core and the Analytic Microscopy Core for their expertise.

Grant Support

This work was sponsored in part by the Moffitt Cancer Center PSOC, NIH/NCI U54CA143970.

The costs of publication of this article were defrayed in part by the payment of page charges. This article must therefore be hereby marked *advertisement* in accordance with 18 U.S.C. Section 1734 solely to indicate this fact.

Received October 28, 2015; revised January 22, 2016; accepted March 7, 2016; published OnlineFirst March 23, 2016.

References

1. Longo DL. Tumor heterogeneity and personalized medicine. N Engl J Med 2012;366:956–7.
2. Gerlinger M, Swanton C. How Darwinian models inform therapeutic failure initiated by clonal heterogeneity in cancer medicine. Br J Cancer 2010;103:1139–43.
3. Sottoriva A, Spiteri I, Piccirillo SG, Touloumis A, Collins VP, Marioni JC, et al. Intratumor heterogeneity in human glioblastoma reflects cancer evolutionary dynamics. Proc Natl Acad Sci U S A 2013;110:4009–14.
4. Yachida S, Jones S, Bozic I, Antal T, Leary R, Fu B, et al. Distant metastasis occurs late during the genetic evolution of pancreatic cancer. Nature 2010;467:1114–7.
5. Greaves M, Maley CC. Clonal evolution in cancer. Nature 2012;481: 306–13.
6. Merlo LM, Pepper JW, Reid BJ, Maley CC. Cancer as an evolutionary and ecological process. Nat Rev Cancer 2006;6:924–35.
7. Gatenby RA, Gillies RJ, Brown JS. Of cancer and cave fish. Nat Rev Cancer 2011;11:237–8.
8. Alfarouk KO, Ibrahim ME, Gatenby RA, Brown JS. Riparian ecosystems in human cancers. Evol Appl 2013;6:46–53.
9. Michelson S, Miller BE, Glicksman AS, Leith JT. Tumor micro-ecology and competitive interactions. J Theor Biol 1987;128:233–46.
10. Aktipis CA, Boddy AM, Gatenby RA, Brown JS, Maley CC. Life history trade-offs in cancer evolution. Nat Rev Cancer 2013;13:883–92.
11. Gatenby RA, Cunningham JJ, Brown JS. Evolutionary triage governs fitness in driver and passenger mutations and suggests targeting never mutations. Nat Commun 2014;5:5499.
12. Brown JS, Pavlovic NB. Evolution in heterogeneous environments: effecs of migration on habitat specialization. Evol Ecol 1992;6:360–82.
13. Morgan PE, Pastorekova S, Stuart-Tilley AK, Alper SL, Casey JR. Interactions of transmembrane carbonic anhydrase, CAIX, with bicarbonate transporters. Am J Physiol Cell Physiol 2007;293:C738–48.
14. Potter CP, Harris AL. Diagnostic, prognostic and therapeutic implications of carbonic anhydrases in cancer. Br J Cancer 2003;89:2–7.
15. Vincent TL, Brown JS. Evolutionary game theory, natural selection, and Darwinian dynamics . Cambridge, UK: Cambridge University Press; 2005.
16. Apaloo J, Brown JS, Vincent TL. Evolutionary game theory: ESS, convergence stability, and NIS. Evol Ecol Res 2009;11:489–515.
17. Cohen Y, Vincent TL, Brown JS. A G-function approach to fitness minima, fitness maxima, evolutionarily stable strategies and adaptive landscapes. Evol Ecol Res 1999;1:923–43.
18. Aktipis CA, Maley CC, Pepper JW. Dispersal evolution in neoplasms: the role of disregulated metabolism in the evolution of cell motility. Cancer Prev Res 2012;5:266–75.
19. Vigueira CC, Olsen KM, Caicedo AL. The red queen in the corn: agricultural weeds as models of rapid adaptive evolution. Heredity 2013;110:303–11.
20. Brown GP, Shilton C, Phillips BL, Shine R. Invasion, stress, and spinal arthritis in cane toads. Proc Natl Acad Sci U S A 2007;104:17698–700.
21. Liebl AL, Martin LB. Living on the edge: range edge birds consume novel foods sooner than established ones. Behav Ecol 2014;25:1089–96.
22. Mitsui H, Suarez-Farinas M, Gulati N, Shah KR, Cannizzaro MV, Coats I, et al. Gene expression profiling of the leading edge of cutaneous squamous cell carcinoma: IL-24-driven MMP-7. J Invest Dermatol 2014;134: 1418–27.
23. Pourreyron C, Reilly L, Proby C, Panteleyev A, Fleming C, McLean K, et al. Wnt5a is strongly expressed at the leading edge in non-melanoma skin cancer, forming active gradients, while canonical Wnt signalling is repressed. PLoS ONE 2012;7:e31827.
24. Georgiou L, Minopoulos G, Lirantzopoulos N, Fiska-Demetriou A, Maltezos E, Sivridis E. Angiogenesis and p53 at the invading tumor edge: prognostic markers for colorectal cancer beyond stage. J Surg Res 2006;131: 118–23.
25. Gatenby RA, Grove O, Gillies RJ. Quantitative imaging in cancer evolution and ecology. Radiology 2013;269:8–15.
26. Zhou M, Hall L, Goldgof D, Russo R, Balagurunathan Y, Gillies R, et al. Radiologically defined ecological dynamics and clinical outcomes in glioblastoma multiforme: preliminary results. Transl Oncol 2014;7:5–13.
27. Gill BJ, Pisapia DJ, Malone HR, Goldstein H, Lei L, Sonabend A, et al. MRI-localized biopsies reveal subtype-specific differences in molecular and cellular composition at the margins of glioblastoma. Proc Natl Acad Sci U S A 2014;111:12550–5.